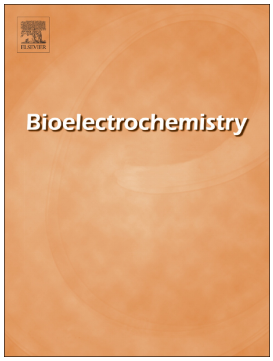

Electrochemical DNA sandwich biosensor based on enzyme amplified microRNA-21 detection and gold nanoparticles

Jihane Mandli, Hasna Mohammadi, Aziz Amine

PII: S1567-5394(16)30259-6
DOI: doi: 10.1016/j.bioelechem.2017.03.002
Reference: BIOJEC 6997

To appear in: *Bioelectrochemistry*

Received date: 29 December 2016
Revised date: 1 March 2017
Accepted date: 12 March 2017

Please cite this article as: Jihane Mandli, Hasna Mohammadi, Aziz Amine , Electrochemical DNA sandwich biosensor based on enzyme amplified microRNA-21 detection and gold nanoparticles. The address for the corresponding author was captured as affiliation for all authors. Please check if appropriate. Biojec(2017), doi: 10.1016/j.bioelechem.2017.03.002

Electrochemical DNA sandwich biosensor based on enzyme amplified microRNA-21 detection and gold nanoparticles

Jihane Mandli, Hasna Mohammadi, Aziz Amine*

Laboratoire Génie des Procédés et Environnement, Faculté de Sciences et Techniques Mohammedia, University Hassan II of Casablanca, Morocco.

*Corresponding author Tel.: +212661454198.
E-mail addresses: azizamine@yahoo.fr, a.amine@univh2m.ac.ma.

Abstract

In this work, a novel electrochemical biosensor for miRNA-21 determination, involving a sandwich hybridization assay onto gold nanoparticles modified pencil graphite electrode (PGE) and enzyme signal amplification was reported.

The thiol terminated capture probe 1 (SH-P1) was immobilized on the electrode through Au–S interaction. In the presence of target miRNA-21, SH-P1 hybridized with the first part of the target, however, the second part hybridizes with a biotinylated probe P2 (B-P2). Then, a streptavidin-conjugated alkaline phosphatase was immobilized by a specific binding of avidin- B-P2. The enzyme catalyzed the electro-inactive α-naphtyl phosphate to an electro-active α-naphtol. The miRNA-21 detection was achieved through the changes of α-naphtol oxidation signals observed at + 0.12 V vs Ag/AgCl with Differential Pulse Voltammetry.

Under the optimal detection conditions, the biosensor exhibited selective and sensitive detection with a linear range from 200 pM to 388 nM and the detection limit was 100 pM (10 fmole in 100 µL).

Keywords: Biosensor; miRNA-21; sandwich hybridization assay; enzyme signal amplification; gold nanoparticles, pencil graphite electrode.

1. Introduction

MicroRNAs (miRNAs) have been discovered for the first time in *Caenorhabditis elegans* [1] and appeared as an important class of short (18-24 nucleotides), single-stranded and non-protein encoding RNAs [2]. Recent studies have confirmed the existence of miRNAs in serum and other body fluids, namely saliva and urine [3]. MicroRNAs have been involved in various biological processes, such as cell differentiation, proliferation and apoptosis [4]. The aberrant expression of miRNAs is generally associated with serious diseases such as cancers, cardiovascular diseases and neurological disorders [5]. Several miRNAs are emerging as novel biomarkers for cancer diagnosis, therapy and prognosis [6].

MicroRNAs represents only 0.01 % of the total mass of RNA [7], therefore any hybridization based-methods are subject to the limitation of potential hybridization of the probe with other RNA. Consequently, fast and inexpensive methods for miRNA detection become more attractive in biological research and clinical diagnosis. The development of such method is still challenging due to the short size, the homology and the low concentrations of miRNAs [8]. For this purpose, various methods have been demonstrated over the past decades, including expensive, complicated and time consuming traditional techniques such as northern blot, reverse transcription polymerase chain reaction (RT-PCR), microarrays and RNA sequencing [9]. Compared to the aforementioned methods, numerous analytical strategies have been developed for miRNA detection, including electrochemical, fluorescent, colorimetric, surface plasmon resonance and electro-chemiluminescent platforms [10]. Though these methods have their own merits, the development of a new detection technologies for miRNA, remains significant challenges in terms of sensitivity, selectivity, simplicity and non-toxic experimental steps [11].

Various amplification strategies have been developed in order to improve the detection sensitivity and adaptability including, nanomaterial amplified assay [12-16] and enzyme-based assay [17-21]. Among these methods, enzymatic amplification is the most commonly used strategy owing to its great simplicity and good reproducibility. However, single amplification by enzyme labels is not sufficient for detecting the ultra-low concentration of miRNAs [22]. These methods mostly require complementary probes labeled by nanoparticles for miRNA recognition [23]. In the enzyme-amplified sensing systems, the enzymatic markers commonly used in connection with electrochemical monitoring of biocatalytic reaction product are; horseradish peroxidase (HRP), glucose oxidase (GOx) and alkaline

phosphatase (ALP) [24-26]. Differing from HRP and GOx, ALP is a non-oxidoreductase that hydrolyzes the substrate to a redox product without an electrochemical activity [27,28].

As far as we know, this is the first report of a simple and sensitive electrochemical miRNA-21 biosensor developed by combining the advantages of enzyme enhancement for signal amplification and sandwich type hybridization performed onto gold nanoparticles (AuNPs) modified pencil graphite electrode (PGE).

The gold nanoparticles displayed a large effective surface area with a good biocompatibility with proteins, DNA and RNA [29] and good electro-conductivity. This allowed more biomolecules (thiol terminated capture probe 1 (SH-P1)) to be immobilized at the electrode surface through Au–S interaction, which reduced the distance for electron transfer and ions diffusion paths between the capture probe and nanomaterials. As a result, the charge transfer to the electrodes became easier. In addition, the strong interactions between capture probe and the electrode surface enhanced the surface density of the immobilized analytes, which therefore leaded to a low detection limit. The developed genosensor avoids the need for previous target labeling which constitutes a very important practical advantage. This genosensor avoids also the need of delicate electrode preparation for control of density and orientation of the recognition probe on the surface and minimizes non-specific adsorptions to allow faster hybridization. The whole strategy is described in this work in connection with the determination of miRNA-21, a potential cancer biomarker up regulated in breast cancer cells, acts as non-specific oncogene, affects tumor invasion and inhibits tumor cell colonization [29,30].

2. Experimental

2.1. Reagents

Streptavidin-alkaline phosphatase-conjugated (SA-AP), α-naphthyl phosphate, chloroauric acid ($HAuCl_4$), diethanolamine (DEA) and 6-mercapto-1-hexanol (MCH) were obtained from Sigma-Aldrich. Magnesium and sodium chloride were purchased from Merck. All other reagents used were of analytical grade.

Throughout this work, ultrapure water has been used.

2.2. Synthetic oligonucleotides

Synthetic oligonucleotides (as lyophilized powder) were purchased from Alpha DNA (Canada) and were used without further purification.

Synthetic oligonucleotides sequences are:

Probe 1: 3'-SH-$(CH_2)_6$-ATCGAATAGT-5'

Probe 2: 3'-GACTACAACT-PolyA10-Biotine-5'

Target miRNA-21: 5'-UAGCUUAUCAGACUGAUGUUGA-3'

Non-complementary has-miRNA-125a:

5'-UCCCUGAGAACCCUUUAACCUGUGA-3'

2.3. Apparatus

Cyclic voltammetry (CV), electrochemical impedance spectroscopy (EIS) and differential pulse voltammetry (DPV) were performed using an electroanalytical instrument (Palmsens BV Houten, Netherlands) in connection with a PC controlled by software PSTrace.

Three electrodes system was employed, consisting of platinum wire as auxiliary electrode, a reference electrode (Ag/AgCl) and 1.67 mm^2 diameter pencil graphite electrode (PGE) as a working electrode. A Rotring T 0.5 pencil was used as holder for the graphite lead (Tombo HB model 0.5 mm). To make the electrical contact with the lead, a metallic wire was soldered to the metal part. The pencil lead was held vertically with 1.5 cm of the lead protruding outside of which 1 cm was immersed inside a glass cell containing 3 mL of the electrolyte.

In order to ensure the reproducibility, the volume of the electrolyte and the position of the electrodes inside the glass cell remain constant throughout the experiments.

2.4. Methods

2.4.1 Electrode pretreatment

For a clean electrode surface, the electrodes were activated by application of +1.40 V for 60 s in unstirred solution of 0.5 M acetate buffer (ABS) containing 20 mM NaCl (pH 4.8).

2.4.2 Modification of pencil graphite electrode by AuNPs

The pretreated clean PGEs were immersed in 0.1 M KNO_3 containing 4 mM $HAuCl_4$ solution. The electrochemical deposition of AuNPs on PGE was carried out between a potential of +0.9V and -0.3 V with a scan rate of 50 $mV.s^{-1}$ as reported in [31]. Followed by a

potential scanning from 0.2 V to 1.6 V in 0.5 M sulfuric acid (H_2SO_4) at a scan rate of 50 $mV.s^{-1}$ until obtaining a reproducible cyclic voltammogram. After washed with phosphate buffred saline (PBS, pH 7.4), the electrodes were dried (noted as AuNPs/PGE).

2.4.3 Probe immobilization

The previously activated AuNPs modified PGEs were immersed in PCR tubes of 200 µL containing 100 µL of 1.1 µM thiol terminated capture probe 1 (SH-P1) and allowed to react overnight at 4 °C, then SH-P1 was immobilized on the electrode by the formation of Au–S bond (noted as SH-P1/AuNPs/PGE). After thoroughly washed with PBS, SH-P1/AuNPs/PGEs were dipped on 100 µL of 1 mM 6-mercapto-1-hexanol (MCH), prepared in 1 M NaCl and 10 mM potassium phosphate buffer, pH 7.0 and incubated for 2 h at 4 °C (noted as MCH/SH-P1/AuNPs/PGE). MCH was used to block the unreacted gold surface, to eliminate the nonspecific adsorption for more efficient hybridization and allows the orientation of the immobilized probes. Again, the electrode was rinsed with PBS.

2.4.4 miRNA-21 hybridization

The hybridization was performed by incubating MCH/SH-P1/AuNPs/PGEs in PCR tubes of 200 µL containing 100 µL of various concentrations of miRNA-21 target (T), for 35 min at room temperature (noted as T/MCH/SH-P1/AuNPs/PGE).

2.4.5 Enzyme interaction

To attach streptavidin-alkaline phosphatase (SA-ALP), the electrode was first allowed to react with 1.1 µM of the biotin labeled probe 2 (B-P2) for 30 min (noted as B-P2/T/MCH/SH-P1/AuNPs/PGE). Thereafter, the resulting electrode was incubated in 12.2 $U.mL^{-1}$ SA-ALP prepared in DEA buffer (1 M, pH 9.8) containing $MgCl_2$ (0.1 M) and BSA (10 $mg.mL^{-1}$) for 30 min. Then, the electrodes were washed with PBS (noted as SA-ALP/B-P2/T/MCH/SH-P1/AuNPs/PGE). Afterwards, the PGEs remain impregnated in DEA buffer until measurement to prevent the surface of the transducer from drying out. For the electrochemical measurements, the resulting electrodes were rinsed with PBS.

2.4.6 Enzyme substrate interaction

Enzyme modified electrodes were exposed to α-naphtyl phosphate (1 $mg.mL^{-1}$ in DEA buffer) at an open circuit potential and under stirring for 10 min.

2.5. Electrochemical measurements

For miRNA sensing, cyclic voltammetry (CV) was carried out in 0.1 M of PBS (pH 7.4) containing 5 mM of $[Fe(CN)_6]^{3-/4-}$ and 0.1 M KCl solution between a potential window of -0.2V and +0.8 V with a scan rate of 100 $mV.s^{-1}$.

Electrochemical impedance spectroscopy (EIS) measurements were performed in PBS containing 5 mM $[Fe(CN)_6]^{3-/4-}$ and 0.1 M KCl solution, with an AC voltage amplitude of 5 mV, a voltage frequencies from 0.1 Hz to 50 kHz and an applied potential of + 0.231 V.

After the interaction of the substrate with the enzyme, the electrochemical oxidation signal of the reaction product of alkaline phosphatase (α-naphtol (α-NAP)), was detected by differential pulse voltammetry (DPV) at + 0.12 V in DEA buffer (pH 9.8) versus Ag/AgCl electrode. The measurements were performed inside an electrochemical cell containing 3 mL of α-naphtyl phosphate.

3. Results and discussion

3.1. Principle of the sandwich hybridization assay

In this work, two single stranded DNA probes: thiol terminated probe 1 and biotin conjugated probe 2 were designed to hybridize with the target miRNA-21. Gold nanoparticles were used to modify PGE for the immobilization of SH-P1 by Au-S bond. AuNPs possess a high surface area and a good biocompatibility [32], thus making them attractive for biosensor preparation and this allows the immobilization of more capture probes SH-P1 at the electrode surface.

To prevent the non-specific adsorption, the empty sites on the SH-P1/AuNP/PGE were blocked with MCH, which has been proven effective in eliminating non-specific adsorption. Then, a part of the target miRNA-21 first hybridizes with SH-P1, subsequently; the other part of the target hybridized with B-P2. Then, with specific interaction between biotin and streptavidin, the SA-ALP was immobilized on B-P2/T/MCH/SH-P1/AuNPs/PGE to catalyze the hydrolysis of substrate (α-naphthyl phosphate) to an electroactive product (α-naphtol (α-

NAP)), which produce an amplified electrochemical signal [33]. The biosensing platform was shown in Schematic 1.

Schematic 1.

3.2. Characterization of the genosensor

Cyclic voltammetry (CV) and electrochemical impedance spectroscopy (EIS) measurements were used in order to characterize the step-by-step modification of the electrode, the measurements were performed on the corresponding electrode in KCl (0.1 M) solution containing the sensitive redox couple of $[Fe(CN)_6]^{3-/4-}$. As displayed in Fig. 1A, a couple of quasi-reversible, well-defined redox peaks of $[Fe(CN)_6]^{3-/4-}$ with a maximum current intensity can be observed on the bare PGE (curve a) due to the excellent electron-transfer kinetics of $[Fe(CN)_6]^{3-/4-}$ to the electrode surface. The current respond increase when PGEs were modified with AuNPs (curve b), this increase could be attributed to the high conductivity of the deposited AuNPs that promote the electron transfer rate. Moreover, AuNPs can further increase the effective surface area and can amplify the signal by their potential to anchor more DNA probes [32]. With the activation of AuNPs/PGE by H_2SO_4 (curve c), the peak currents sharply increased, which was attributed to the acceleration of the electron transfer. However, as shown in Fig.1B, the current response decrease greatly after immobilization of SH-P1 (1.1 µM) (curve d), which could be explained by the negatively charged orthophosphate backbone of the probe that repelled the negatively charged $[Fe(CN)_6]^{3-/4-}$ and inhibit the electron transfer. This also proved that SH-P1 had been successfully immobilized on the electrode. The redox currents gradually increase when the SH-P1/AuNPs/PGEs were reacted with 1 mM of 6-mercapto-1-hexanol (MCH) (curves e), which linked the probe to the electrode via six-carbon linker and remains flexible enough to transfer electrons. Additionally, the peak currents further decrease after hybridization of capture probe with 1.5 µM miRNA-21 target (curve f). This decrease in signal was attributed to the electrostatic repulsive-force between phosphate skeleton of DNA–RNA hybrids and the redox couple of $[Fe(CN)_6]^{3-/4-}$. The CV results suggested the successful construction of the biosensor. These results were in a good agreement with those obtained from EIS measurements (Fig. 1C/D), in which the electron transfer resistance (Ret) varied upon the assembly and binding processes.

Fig.1

3.3. Optimization of the detection conditions

Several experimental conditions were optimized to obtain good analytical performance. Because the aim of this work is to determine miRNA-21 based on signal amplification using thiol terminated capture probe immobilized on AuNPs-PGE, the probe immobilization amount can direct influence the determination sensitivity. Thus, we immobilized the probe onto AuNPs-PGE. The use of AuNPs as biosensing platform can be attributed to two aspects. One is that AuNPs possesses excellent conductivity, which can increase the electrochemical response of α-NAP. The other is that AuNPs has a high specific surface area and can increase the electrode effective surface area, so AuNPs can be electrochemically deposited on the electrode surface to assemble more probe molecules. For confirming this, the effect of deposition of AuNPs by CV was tested in the range of 5-20 scans (Fig.2A). The highest current response 210 µA was obtained after six deposition scans. So six scans of AuNPs deposition were used for the rest of the work. Also, the electrode effective surface area was determined based on the oxido-reduction peak area of AuNPs when the electrode was immersed in 0.5 M H_2SO_4 and scanned from 0.2 to 1.6 V by cyclic voltammetry. As shown in Fig.2B the peak current increases when the activation of AuNPs by H_2SO_4 was occurred at five scans, and the oxidation peak current reached 225 µA indicating the utility of AuNPs for improving the detection sensitivity. Thus, five scans for activation of AuNPs were used.

Fig.2

The optimum concentration of thiol terminated capture probe 1 was determined based on the changes at the peak current value obtained by CV (Fig. 3). Therefore, different concentrations ranging from 0.2 to 7.6 µM were immobilized on AuNPs/PGEs for overnight at 4°C. Then, the hybridization between miRNA-21 target (1.5 µM) and its complementary probe SH-P1 at different concentrations was performed. The changes at the peak current value obtained by CV after hybridization process were compared to the ones obtained in the presence of only thiol terminated capture probe 1. The average of current recorded with SH-P1/AuNPs/PGE was 283.2 µA (RSD % = 6.6 %, n = 4) after immobilization of SH-P1 (1.1 µM) on AuNPs/PGEs, (Fig. 3-MCH/SH-P1/AuNPs/PGE). A significant decrease at the peak current value was obtained after hybridization of miRNA-21 target (1.5 µM) and SH-P1/AuNPs/PGE (1.1 µM) (Fig. 3-T/MCH/SH-P1/AuNPs/PGE) and the peak current measured was 215.9 µA

with an RSD % = 3.5 % (n = 4). This decrease in signal can be attributed to the immobilization of double-stranded DNA–RNA hybrids, which induce a decrease in repulsive interaction between anionic redox couple of $Fe(CN)_6^{4-/3-}$ and the electrode surface [34]. According to the CV results, 1.1µM was chosen as an optimum concentration of thiol-terminated capture probe 1.

Fig.3

We also investigated the effect of SA-ALP concentrations according to α-NAP oxidation signal with DPV. As shown in Fig.4, the peak current increases rapidly when the concentration of ALP increases from 0.1 to 12.2 $U.mL^{-1}$ and the best response was obtained with 12.2 $U.mL^{-1}$ of ALP allowing to a high oxidation of α-NAP. In order to reduce the cost of the assay, concentrations higher than 12.2 $U.mL^{-1}$ of ALP were not tested.

Other parameters affecting the hybridization were also optimized such as; hybridization buffer, temperature and hybridization time, and were specified for the best analytical performances. All the conditions listed in Table 1 and the optimum conditions (last column, bold) were determined according to α-NAP oxidation signal ratio obtained for probe and hybrid. The best conditions were used for the rest of the work.

Fig.4

3.4. Analytical performances of the sandwich hybridization assay

In this work, signal enhancement is implemented by binding streptavidin-alkaline phosphatase to the biotin conjugated probe 2. Since, the streptavidin has a high affinity to the biotin, the enzyme was expected to govern the oxidation reaction when the hybridization occurs, by measuring the catalytic current generated by the electrochemical oxidation of α-NAP. On the other hand, without target miRNA-21, the sandwich complex is not formed and the surface confined capture probe remains un-hybridized. Fig.5 depicts the changes in α-NAP oxidation signals after hybridization. As it is clear from these results, the oxidation signal of α-NAP observed at +0.12 V versus Ag/AgCl nearly corresponds to the signals recorded for α-NAP [35]. However, there is a dramatic increase in the α-NAP signal observed with increasing concentration of miRNA-21.

According to the results of optimization study and the calibration plot drawn accordingly, the changes of the α-NAP oxidation signals were proportional to the logarithm of miRNA-21 concentrations in the range of 200 pM to 388 nM with a correlation coefficient of 0.987. The regression equation was I (μA) = 0.85 log C + 1.83, where C corresponds to μA/nM, the limit of detection was 100 pM (S/N=3) which correspond to 10 fmole miRNA-21 in 100 μL. This value was obtained without the use of PCR as an amplification technique. The sensitivity of the genosensor might be attributed to two factors. First, is the strong interactions between thiol conjugated capture probes and AuNPs modified PGE that enhanced the surface density of the immobilized analytes, leading to a greater quantity of miRNA-21 target that can be bound by SH-P1. Second, is that each SA-ALP can catalyze the production of a large number of electrochemically active molecules due to its high turnover and high reaction selectivity.

The developed miRNA-21 biosensor was quite easier and requires less experimental steps compared to other reports based on sandwich hybridization assay [27,36,37]. The proposed sandwich hybridization method showed a better performances in terms of analytical range and detection limit than other electrochemical biosensors employed for miRNA detection, namely, a magneto-biosensor [11], a multi-channel screen printed electrodes [13], an osmium (VI) complex for miRNA 3′-end labeling [38], a tryptophan inside p19 [39]. Up to date, one reported method was demonstrated by using enzyme amplification and PGE for miRNA determination [21]. However, this similar strategy present stringency drawbacks, namely, the low sensitivity (1 μM), the biosensor requires high concentration of probe (5 $\mu g.mL^{-1}$) and enzyme (1 $mg.mL^{-1}$) and labeled miRNAs since they cannot be applied directly for real sample analysis unless specific and expensive kit to perform the analysis was employed. Also during real samples analysis the biosensor requires more steps and complex working protocols, which increases the cost. In order to overcome these limitations, the developed genosensor have been developed with high selectivity and sensitivity with its picomolar detection limit. Besides the low limit of detection of the biosensor, it is important to mention that the approach reported here did not require sophisticated instruments and obviated the use of previous target labeling, reducing the cost and the complexity of the assays.

According to previous reported study [21], the minimum detectable miRNA-21 concentration in total RNA extracted from human breast cells (MCF-7) is 150 nM which correspond to 15 pmole miRNA-21 in 100 μL [21]. Under our experimental conditions, the detection limit is 100 pM (10 fmole miRNA-21 in 100 μL). Thus, our biosensor is more sensitive and can be used for a possible follow-up of the progression of breast cancer (biopsies) and would be a promising method in clinical and biomedical applications. Indeed, miRNA-21 is known to be

up-regulated and the concentration is expected to be higher in extract obtained from person suffering from breast cancer [29,40].

Fig.5

3.5. Selectivity and reproducibility of the sandwich hybridization assay

3.5.1. Selectivity

The selectivity of the fabricated biosensor in discriminating completely complementary target miRNA-21 from non-complementary miRNA-125a sequence was investigated under the concentration of 0.6 µM.

MicroRNA-125a was assayed as the non-complementary sequence because it also appears up regulated in breast cancer [40] but its sequence differs markedly from miRNA-21 target. As shown in Fig. 6, the higher peak current is obtained for the complementary miRNA-21 target and the peak current of miRNA-125a almost remained absent, indicating that SH-P1 did not hybridize with miRNA-125a. These results demonstrated the high selectivity of the proposed approach to discriminate the target miRNA-21 over non-complementary target.

Fig.6

3.5.2. Reproducibility

The reproducibility of the proposed miRNA-21 biosensor was also investigated. Four parallel made T-P2/MCH/SH-P1/AuNPs/PGEs were used to detect different concentrations of miRNA-21 (0.2, 0.7, 2, 7, 23, 75, 388 and 755 nM). The relative standard deviation (RSD) value obtained (n = 4) was respectively 2.1, 3.5, 9.9, 2.2, 4.5, 3.8, 6.6 and 2.4 %, indicating that multiple electrodes can be prepared concurrently for the assays of many different samples. These results revealed the good level of precision achieved in the fabrication and functioning of the proposed genosensor device.

4. Conclusions

In the present study, we report simple, sensitive and disposable electrochemical biosensor for microRNAs determination. The developed genosensor was based on AuNPs modified PGE coupling with thiol terminated probe and enzyme signal amplification involving a sandwich hybridization assay with several advantages. First, the large specific area of gold nanoparticles that provided a promising sensing platform. Second, the strong interaction between thiol conjugated capture probe and AuNPs allows the good capture of miRNA-21 target. Third, is that each SA-ALP can catalyze the production of a large amount of electrochemically active molecules. Finally, the established miRNA assay exhibited a high sensitivity with a low limit of detection 100 pM (10 fmole in 100 µL) in 45 min (once SH-P1/AuNPs/PGE is prepared) and a good selectivity and reproducibility.

Acknowledgements

Authors would like to acknowledge Professor Mehmet Özsöz and his team of research in Gediz University, Turkey, for the fruitful discussion and partial support of this work.

References

[1] B. Wightman, I. Ha, G. Ruvkun, Posttranscriptional regulation of the heterochronic gene lin-14 by lin-4 mediates temporal pattern formation in C, Elegans. Cell. 75 (1993) 855-862.

[2] B. Li, F. Liu, Y. Peng, Y. Zhou, W. Fan, H. Yin, X. Zhang, Two-stage cyclic enzymatic amplification method for ultrasensitive electrochemical assay of microRNA-21 in the blood serum of gastric cancer patients, Biosens. Bioelectron. 79 (2016) 307-312.

[3] W. Ma, B. Situ, W. Lv, B. Li, X. Yin, P. Vadgama, W. Wang, Electrochemical determination of microRNAs based on isothermal strand-displacement polymerase reaction coupled with multienzyme functionalized magnetic micro-carriers, Biosens. Bioelectron. 80 (2016) 344-351.

[4] Z. Lu, H. Tang, D. Wu, Y. Xia, M. Wu, X. Yi, J. Wang, Amplified voltammetric detection of miRNA from serum samples of glioma patients via combination of conducting magnetic microbeads and ferrocene-capped gold nanoparticle/streptavidin conjugates, Biosens. Bioelectron. 86 (2016) 502-507.

[5] X. Li, W. Cheng, D. Li, J. Wu, X. Ding, Q. Cheng, S. Ding, A novel surface plasmon resonance biosensor for enzyme-free and highly sensitive detection of microRNA based on multi component nucleic acid enzyme (MNAzyme)-mediated catalyzed hairpin assembly, Biosens. Bioelectron. 80 (2016) 98-104.

[6] H. Zhou, C. Yang, H. Chen, X. Li, Y. Li, X. Fan, A simple G-quadruplex molecular beacon-based biosensor for highly selective detection of microRNA, Biosens. Bioelectron. 87 (2017) 552-557.

[7] J. Krol, I. Loedige, W. Filipowicz, The widespread regulation of microRNA biogenesis, function and decay, Nat. Rev. Genet. 11 (2010) 597-610.

[8] C.-Y. Hong, X. Chen, T. Liu, J. Li, H.-H. Yang, Chen, J.-H., G.-N. Chen, Ultrasensitive electrochemical detection of cancer-associated circulating microRNA in serum samples based on DNA concatamers, Biosens. Bioelectron. 50 (2013)132-136.

[9] J.-b. Li, P. Lei, S. Ding, Y. Zhang, J. Yang, Q. Cheng, Y. Yan, An enzyme-free surface plasmon resonance biosensor for real-time detecting microRNA based on allosteric effect of mismatched catalytic hairpin assembly, Biosens. Bioelectron. 77 (2016) 435-441.

[10] X. Miao, W. Wang, T. Kang, J. Liu, K.-K. Shiu, C.-H. Leung, D.-L. Ma, Ultrasensitive electrochemical detection of microRNA by using an iridium (III) complex as catalyst, Biosens. Bioelectron. 86 (2016) 454-458.

[11] R.-M. Torrente-Rodríguez, S. Campuzano, E. López-Hernández, V.-R.-V. Montiel, R. Barderas, R. Granados, J.-M. Pingarrón, Simultaneous detection of two breast cancer-related miRNAs in tumor tissues using p19-based disposable amperometric magnetobiosensing platforms, Biosens. Bioelectron. 66 (2015) 385-391.

[12] B. Jin, P. Wang, H. Mao, B. Hu, H. Zhang, Z. Cheng, Q. Jin, Multi-nanomaterial electrochemical biosensor based on label-free graphene for detecting cancer biomarkers, Biosens. Bioelectron. 55 (2014) 464-469.

[13] A. Erdem, G. Congur, Label-free voltammetric detection of MicroRNAs at multi-channel screen printed array electrodes comparison to graphite sensors, Talanta. 118 (2014) 7-13.

[14] W. Zhu, X. Su, X. Gao, Z. Dai, X. Zou, A label-free and PCR-free electrochemical assay for multiplexed microRNA profiles by ligase chain reaction coupling with quantum dots barcodes, Biosens. Bioelectron. 53 (2014) 414-419.

[15] X. Wu, Y. Chai, R. Yuan, H. Su, J. Han, A novel label-free electrochemical microRNA biosensor using Pd nanoparticles as enhancer and linker, Analyst. 138 (2013) 1060-1066.

[16] N. Xia, L. Zhang, G. Wang, Q. Feng, L. Liu, Label-free and sensitive strategy for microRNAs detection based on the formation of boronate ester bonds and the dual-amplification of gold nanoparticles, Biosens. Bioelectron. 47 (2013) 461-466.

[17] C. Yang, B. Dou, K. Shi, Y. Chai, Y. Xiang, R. Yuan, Multiplexed and amplified electronic sensor for the detection of microRNAs from Cancer Cells, Anal. Chem. 86 (2014) 11913-11918.

[18] C. Jamesáyang, A T7 exonuclease-assisted cyclic enzymatic amplification method with rolling circle amplification: a dual-amplification strategy for sensitive and selective microRNA detection, Chem. Commun. 50 (2014) 1576-1578.

[19] M. Wang, Z. Fu, B. Li, Y. Zhou, H. Yin, S. Ai, One-step, ultrasensitive, and electrochemical assay of microRNAs based on T7 exonuclease assisted cyclic enzymatic amplification, Anal. Chem. 86 (2014) 5606-5610.

[20] G. Xiang, D. Jiang, F. Luo, F. Liu, L. Liu, X. Pu, Sensitive detection of microRNAs using hemin/G-quadruplex conctamers as trace labels and RNA endonuclease-aided target recycling for amplification, Sensor. Actuat. B-Chem. 195 (2014) 515-519.

[21] T. Kilic, S.-N. Topkaya, D.-O. Ariksoysal, M. Ozsoz, P. Ballar, Y. Erac, O. Gozen, Electrochemical based detection of microRNA, mir21 in breast cancer cells, Biosens. Bioelectron. 38 (2012) 195-201.

[22] H.-L. Shuai, K.-J. Huang, L.-L. Xing, Y.-X. Chen, Ultrasensitive electrochemical sensing platform for microRNA based on tungsten oxide-graphene composites coupling with catalyzed hairpin assembly target recycling and enzyme signal amplification, Biosens. Bioelectron. 86 (2016) 337-345.

[23] L. Liu, N. Xia, H. Liu, X. Kang, X. Liu, C. Xue, X. He, Highly sensitive and label-free electrochemical detection of microRNAs based on triple signal amplification of multifunctional gold nanoparticles, enzymes and redox-cycling reaction, Biosens. Bioelectron. 53 (2014) 399-405.

[24] Z. Gao, A highly sensitive electrochemical assay for microRNA expression profiling, Analyst. 137 (2012) 1674-1679.

[25] Y. Wen, H. Pei, Y. Shen, J. Xi, M. Lin, N. Lu, C. Fan, DNA nanostructure-based interfacial engineering for PCR-free ultrasensitive electrochemical analysis of microRNA, Sci. Rep. 2 (2012) 867.

[26] H. Yang, Enzyme-based ultrasensitive electrochemical biosensors, Curr. Opin. Chem. Biol. 16 (2012) 422-428.

[27] X. Ding, Y.-Yan, S. Li, Y. Zhang, W. Cheng, Q. Cheng, S. Ding, Surface plasmon resonance biosensor for highly sensitive detection of microRNA based DNA super-sandwich assemblies and streptavidin signal amplification, Anal. Chim. Acta. 874 (2015) 59-65.

[28] N. Xia, Y. Zhang, X. Wei, Y. Huang, L. Liu, An electrochemical microRNAs biosensor with the signal amplification of alkaline phosphatase and electrochemical–chemical–chemical redox cycling, Anal. Chim. Acta. 878 (2015) 95-101.

[29] M. Kaplan, T. Kilic, G. Guler, J. Mandli, A. Amine, M. Ozsoz, A novel method for sensitive microRNA detection: Electropolymerization based doping, Biosens. Bioelectron. (2016). DOI: 10.1016/j.bios.2016.09.050.

[30] A. Usmani, A.-A. Shoro, Z. Memon, M. Hussain, R. Rehman, Diagnostic, prognostic and predictive value of microRNA-21 in breast cancer patients, their daughters and healthy individuals. Am. J. Canc. R. 5 (2015) 2484.

[31] S.-F. Liu, X.-H. Li, Y.-C. Li, Y.-F. Li, J.-R. Li, L. Jiang, The influence of gold nanoparticle modified electrode on the structure of mercaptopropionic acid self-assembly monolayer, Electrochim. Acta. 51 (2005) 427-431.

[32] H. Yin, Y. Zhou, H. Zhang, X. Meng, S. Ai, Electrochemical determination of microRNA-21 based on graphene, LNA integrated molecular beacon, AuNPs and biotin multifunctional bio bar codes and enzymatic assay system, Biosens. Bioelectron. 33 (2012) 247-253.

[33] Q. Zhai, Y. He, X. Li, J. Guo, S. Li, G. Yi, A simple and ultrasensitive electrochemical biosensor for detection of microRNA based on hybridization chain reaction amplification, J. Electroanal. Chem. 758 (2015) 20-25.

[34] L. Liu, S. Jiang, L. Wang, Z. Zhang, G. Xie, Direct detection of microRNA-126 at a femtomolar level using a glassy carbon electrode modified with chitosan, graphene sheets, and a poly (amidoamine) dendrimer composite with gold and silver nanoclusters, Microchim. Acta. 182 (2015) 77-84.

[35] M. Wang, B. Shen, R. Yuan, W. Cheng, H. Xu, S. Ding, An electrochemical biosensor for highly sensitive determination of microRNA based on enzymatic and molecular beacon mediated strand displacement amplification, J. Electroanal. Chem. 756 (2015) 147-152.

[36] R. M. Torrente-Rodríguez, S. Campuzano, V.-R.-V. Montiel, J.-J. Montoya, J.-M. Pingarrón, Sensitive electrochemical determination of miRNAs based on a sandwich assay onto magnatic microcarriers and hybridization chain reaction amplification. Biosens. Bioelectron. 86 (2016) 516-521.

[37] Y. Wen, G. Liu, H. Pei, L. Li, Q. Xu, W. Liang, C. Fan, DNA nanostructure-based ultrasensitive electrochemical microRNA biosensor. Methods. 64 (2013) 276-282.

[38] M. Bartosik, R. Hrstka, E. Palecek, B. Vojtesek, Magnetic bead-based hybridization assay for electrochemical detection of Magnetic bead-based hybridization assay for electrochemical detection of microRNA, Anal. Chim. Acta. 813 (2014) 35-40.

[39] T. Kilic, S.-N. Topkaya, M. Ozsoz, A new insight into electrochemical microRNA detection: a molecular caliper, p19 protein, Biosens. Bioelectron. 48 (2013) 165-171.

[40] J. Le Quesne, C. Caldas, Micro-RNAs and breast cancer, Mol. Oncol. 4 (2010) 230-241.

Figure Captions

Schematic 1. Depicts the principle of the electrochemical biosensor for miRNA-21 detection.

Fig.1 Cyclic voltammograms (A, B) and impedance measurements (C, D) of bare PGE (a), AuNPs/GCE (b), activated AuNPs/GCE (c) SH-P1/AuNPs/GCE (d), MCH/SH-P1/AuNPs/PGE (e), T/MCH/SH-P1/AuNPs/PGE (f). Experimental conditions: electrode pretreatment; + 1.40 V for 60 s in 0.5 M ABS (pH 4.8), electrochemical deposition of AuNPs; + 0.9 V and - 0.3 V in 0.1 M KNO_3 and 4 mM $HAuCl_4$, 0.2 V to 1.6 V in 0.5 M H_2SO_4. Probe immobilization; 1.1 µM SH-P1 immobilized on AuNPs/PGEs for overnight at 4 °C. Hybridization; 1.5 µM miRNA-21 immobilized on MCH/SH-P1/AuNPs/PGEs for 35 min. CV and EIS measurement; - 0.2 V to + 0.8 V in 5 mM $[Fe(CN)_6]^{3-/4-}$ and 0.1 M KCl.

Fig.2 Histograms with error bars showing the deposition effect of AuNPs (A) and the activation of AuNPs by H_2SO_4 (B). Experimental conditions: electrode pretreatment; + 1.4 V for 60 s in 0.5 M ABS (pH 4.8), electrochemical deposition of AuNPs; + 0.9 V and - 0.3 V in 0.1 M KNO_3 and 4 mM $HAuCl_4$, + 0.2 V to 1.6 V in 0.5 M H_2SO_4. CV measurement; - 0.2 V to + 0.1 V in 5 mM $[Fe(CN)_6]^{3/4}$ and 0.1 M KCl.

Fig.3 Probe optimization Histograms with error bars of different probe concentrations (0.5-1.3 µM) with 1.5 µM miRNA-21 target. Experimental conditions: electrode pretreatment; + 1.4 V for 60 s in 0.5 M ABS (pH 4.8), electrochemical deposition of AuNPs; + 0.9 V and - 0.3 V in 0.1 M KNO_3 and 4 mM $HAuCl_4$, 0.2 V to 1.6 V in 0.5 M H_2SO_4. Probe immobilization; SH-P1 was immobilized on AuNPs/PGEs for overnight at 4 °C. Hybridization; miRNA-21 was immobilized on SH-P1/AuNPs/PGEs for 35 min. CV measurement; - 0.2 V to + 0.8 V in 5 mM $[Fe(CN)_6]^{3/4}$ and 0.1 M KCl.

Fig.4 Differential pulse voltammograms for α-NAP oxidation signals recorded after hybridization by increasing the concentration of SA-ALP. Experimental conditions: electrode pretreatment; + 1.4 V for 60 s in 0.5 M ABS (pH 4.8), electrochemical deposition of AuNPs; +0.9 V and - 0.3 V in 0.1 M KNO_3 and 4 mM $HAuCl_4$, 0.2 V to 1.6 V in 0.5 M H_2SO_4. Probe immobilization; 1.1 µM SH-P1 immobilized on AuNPs/PGEs for overnight at 4 °C. Hybridization; 0.4 µM miRNA-21 immobilized on MCH/SH-P1/AuNPs/PGEs for 35 min and B-P2/MCH/T/SH-P1/AuNPs/PGE was incubated in SA-ALP for 30 min. DPV measurement; - 0.4 to + 0.6 V in 1 $mg.mL^{-1}$ α-naphtyl phosphate in DEA buffer.

Fig.5 Differential pulse voltammograms of different concentrations of miRNA-21 target. Experimental conditions: electrode pretreatment; + 1.4 V for 60 s in 0.5 M ABS (pH 4.8), electrochemical deposition of AuNPs; + 0.9 V and - 0.3 V in 0.1 M KNO_3 and 4 mM $HAuCl_4$, 0.2 V to 1.6 V in 0.5 M H_2SO_4. Probe immobilization; 1.1 µM SH-P1 was immobilized on AuNPs/PGEs for overnight at 4 °C. Hybridization; miRNA-21 (0.2-755 nM) immobilized on MCH/SH-P1/AuNPs/PGEs for 35 min. T/MCH/SH-P1/AuNPs/PGEs reacted with 1.1 µM of B-P2 for 30 min, then, B-P2/MCH/T/SH-P1/AuNPs/PGEs were incubated in 12.2 $U.mL^{-1}$ SA-ALP for 30 min. DPV measurement; - 0.4 to + 0.6 V in 1 $mg.mL^{-1}$ α-naphtyl phosphate in DEA buffer.

Fig.6 Differential pulse voltammograms of selectivity study of the genosensor against: non-complementary sequence miRNA-125 (a), and target miRNA-21 (b). Experimental conditions: electrode pretreatment; + 1.4V for 60s in 0.5 M ABS (pH 4.8), electrochemical deposition of AuNPs; + 0.9 V to - 0.3 V in 0.1 M KNO_3 and 4 mM $HAuCl_4$, 0.2 V to 1.6 V in 0.5 M H_2SO_4. Probe immobilization; SH-P1 immobilized in AuNPs/PGEs for overnight at 4 °C. Hybridization; 0.6 µM miRNA-21/miRNA-125a immobilized in MCH/SH-P1/AuNPs/PGEs for 35 min. NC or T/MCH/SH-P1/AuNPs/PGEs reacted with 1.1 µM B-P2 for 30 min, B-P2/MCH/T/SH-P1/AuNPs/PGE were incubated in 12.2 $U.mL^{-1}$ SA-ALP for 30 min. DPV measurement; - 0.4 to + 0.60 V in 1 $mg.mL^{-1}$ α-naphtyl phosphate in DEA buffer.

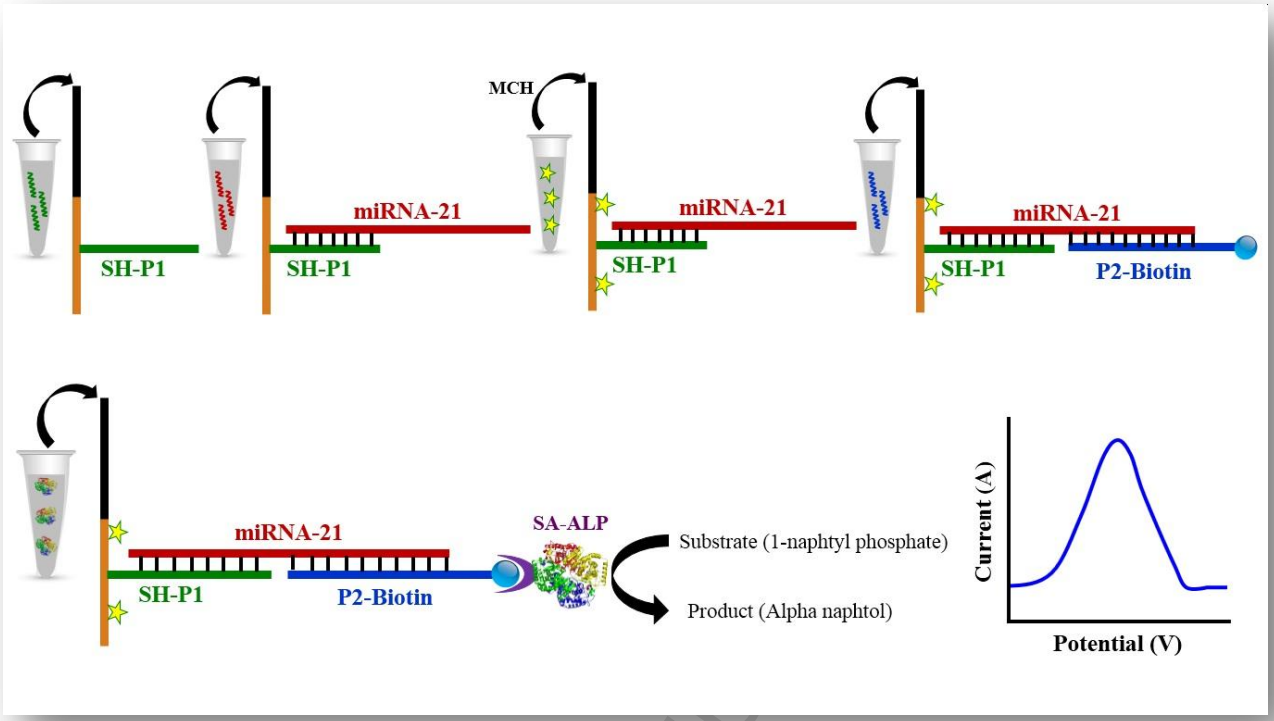

Schematic 1.

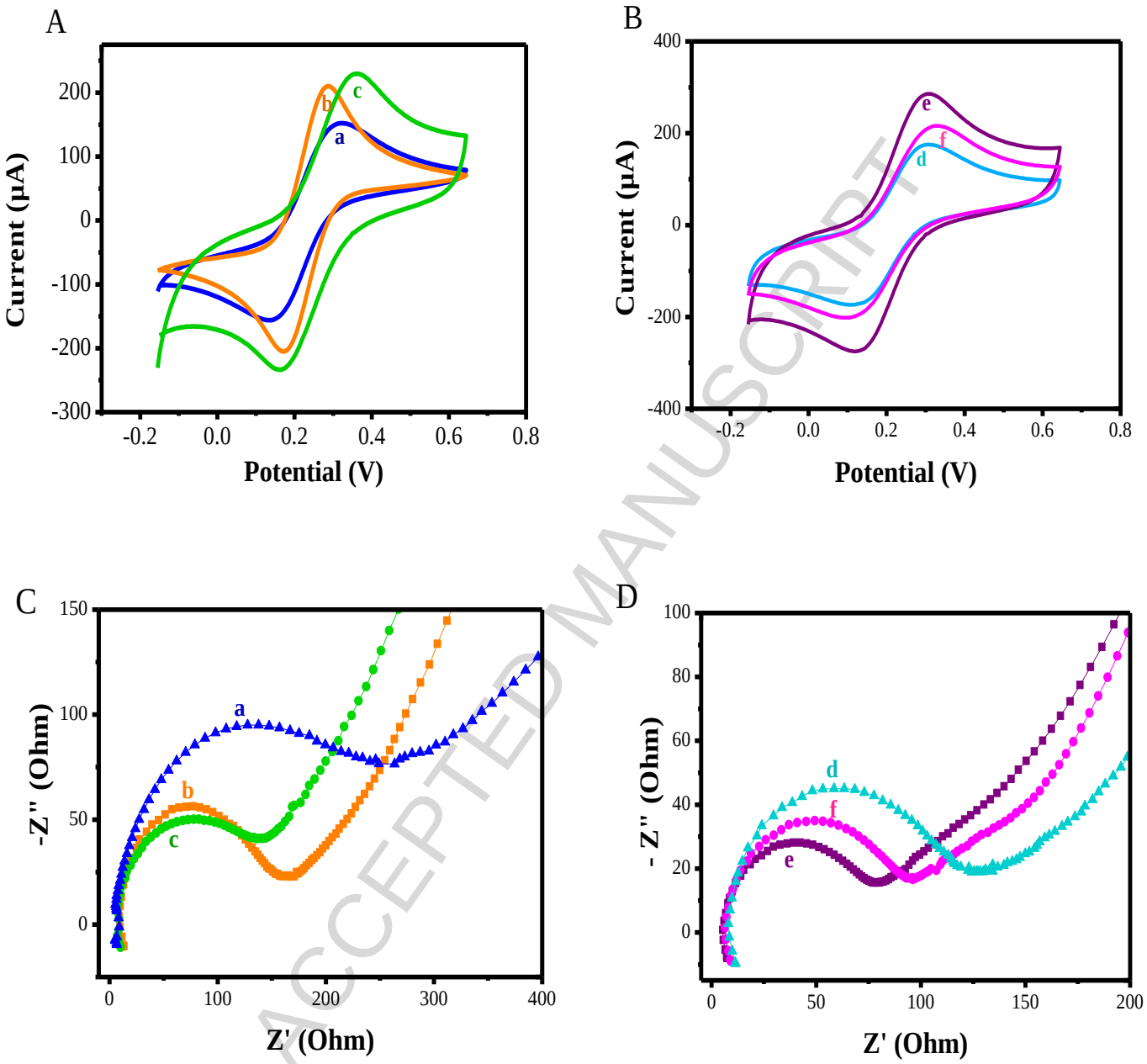

Fig.1.

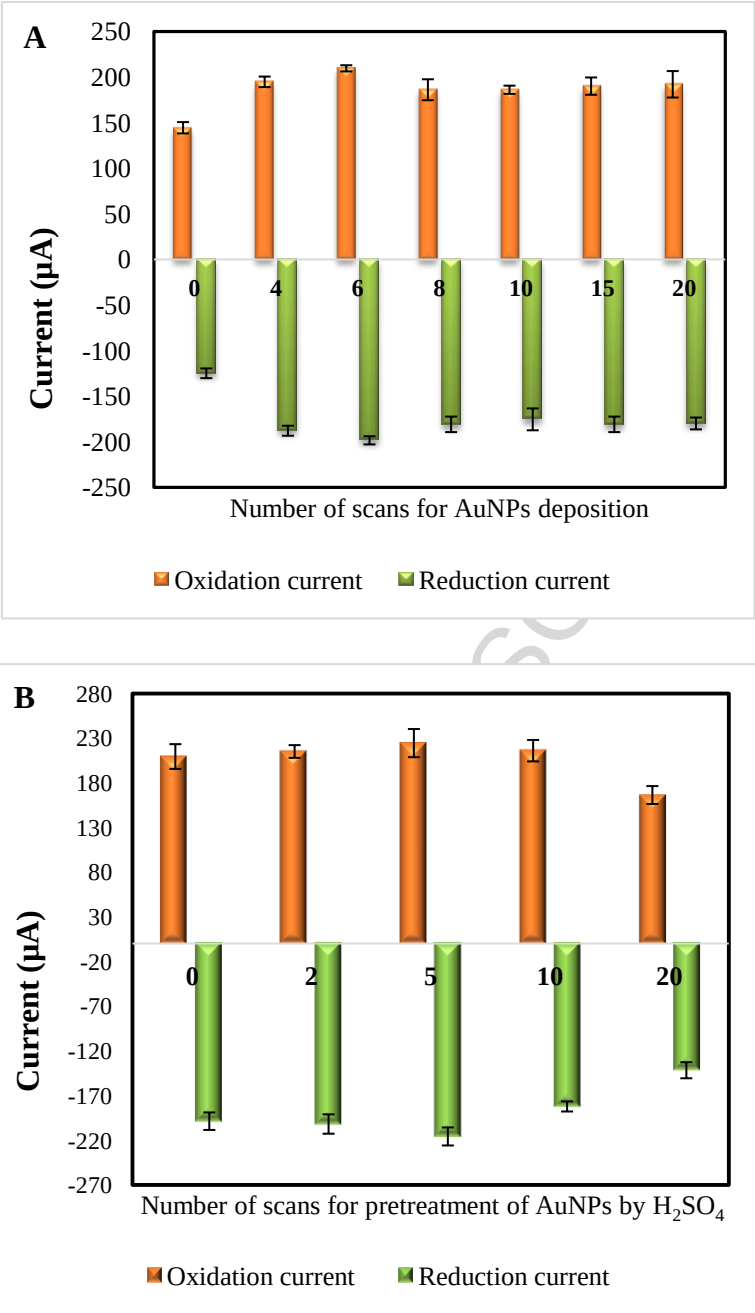

Fig.2.

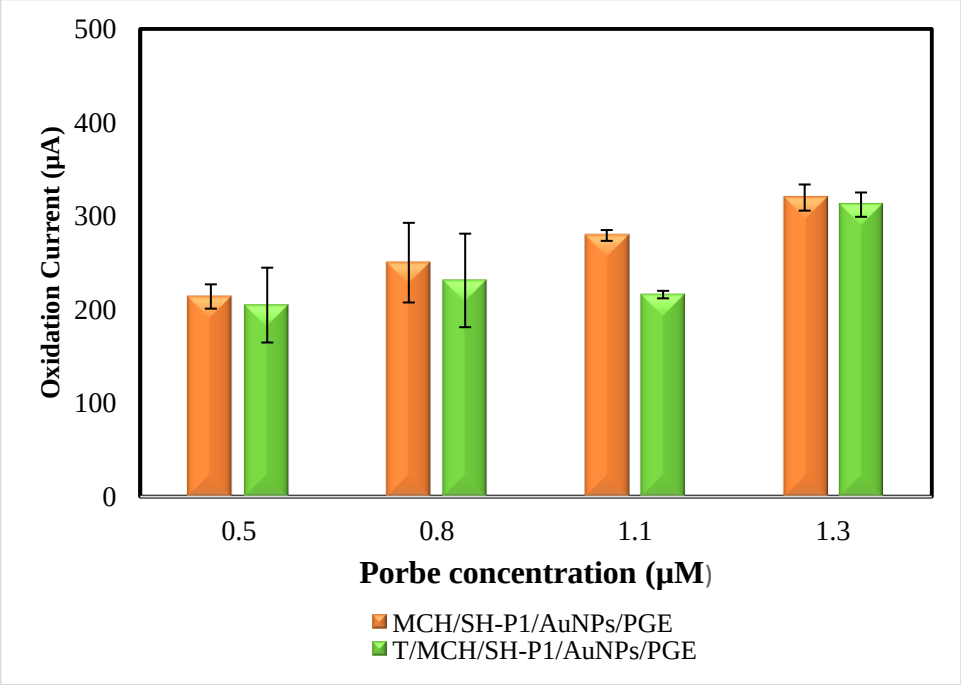

Fig.3.

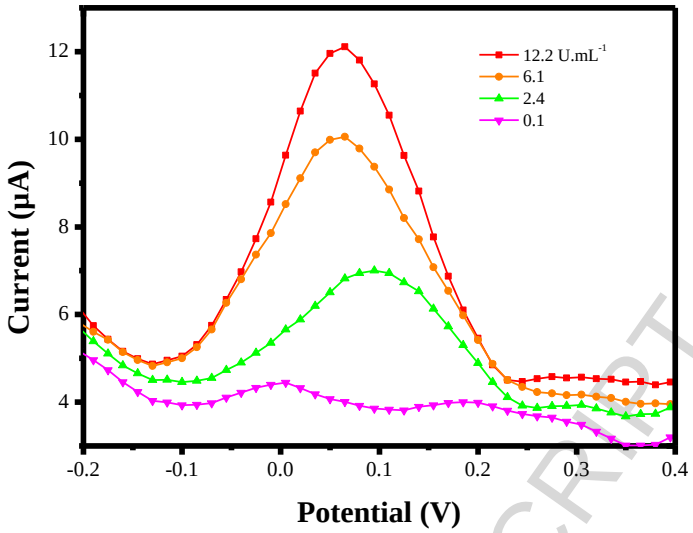

Fig.4.

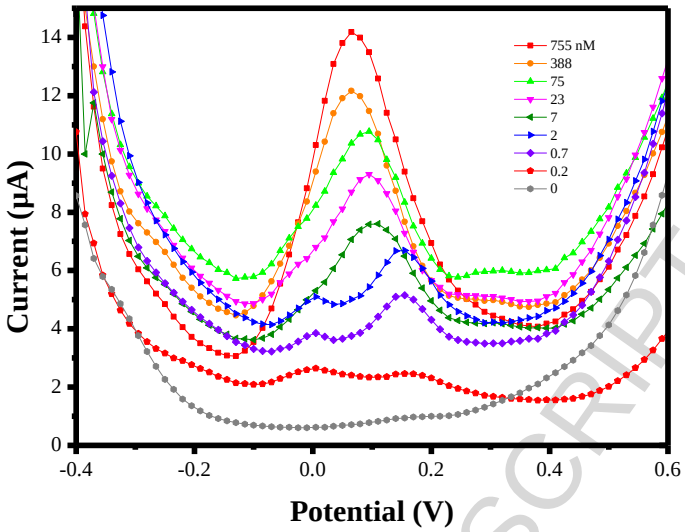

Fig.5.

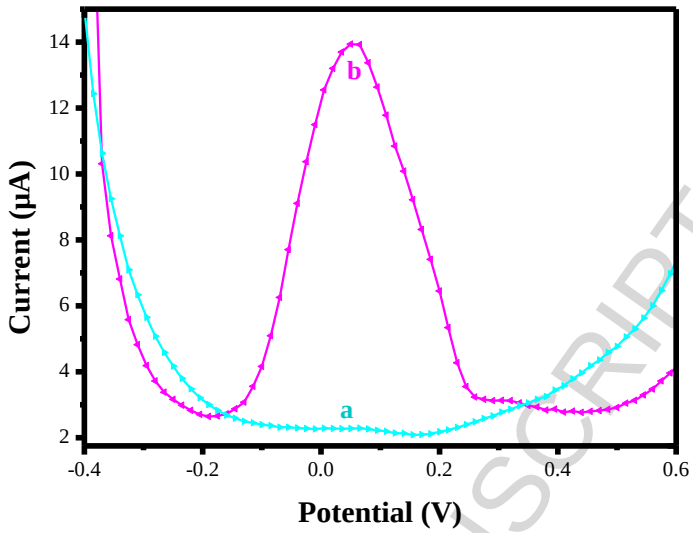

Fig.6

Table.1 Optimization of different experimental variables affecting the hybridization of miRNA-21.

Variable	Range Tested	Selected Value
Hybridization Buffer	DEA pH 9.8 Tris pH 9.0	DEA buffer pH 9.8
Hybridization Temperature (°C)	4, 26	26
Hybridization Time (min)	120, 60, 35	35
SH-P1 (µM)	0.2 to 7.6	1.1
SA-ALP ($U.ML^{-1}$)	0.1 to 12.2	12.2

Graphical abstract

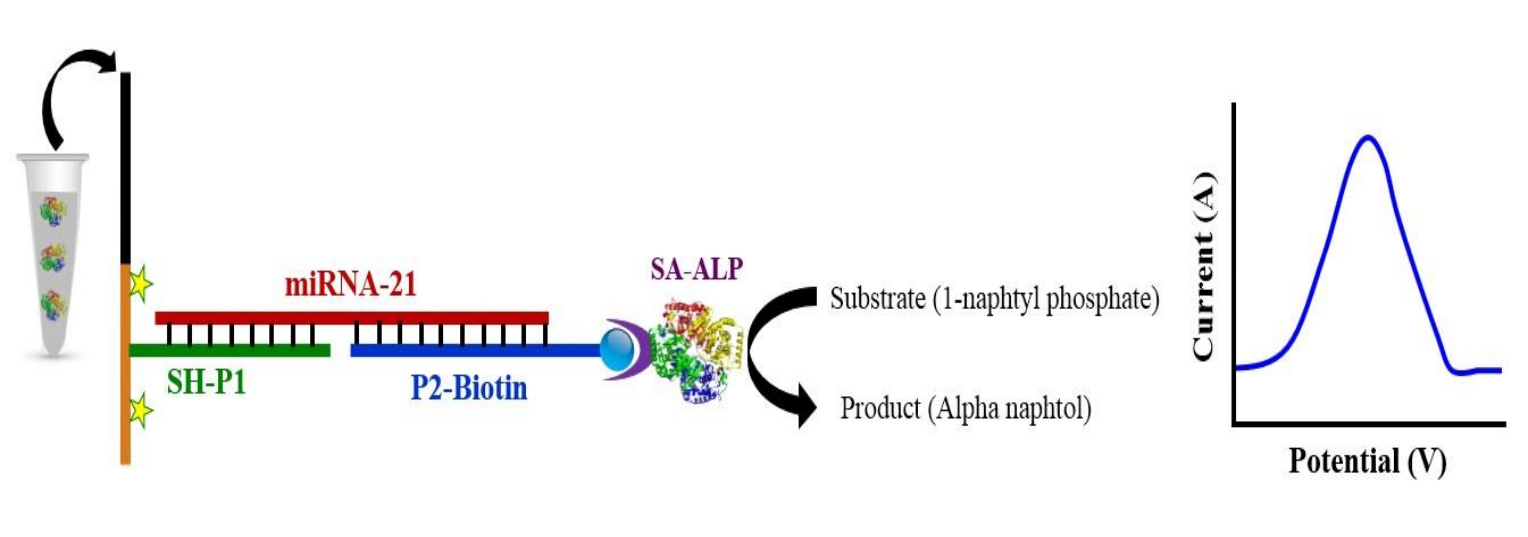

Highlights

- Electrochemical biosensor for simple and fast miRNAs determination was developed.
- Pencil graphite electrode modified with gold nanoparticles was used as biosensing platform.
- Sandwich hybridization assay with enzyme signal amplification was developed.
- 100 pM (10 fmol in 100 μL) for the target miRNA-21 was detected.